

Scientific Article

# Brain metastases with poor vascular function are susceptible to pseudoprogression after stereotactic radiation surgery

Ingrid Digernes MSc <sup>a,\*</sup>, Endre Grøvik PhD <sup>a</sup>, Line B. Nilsen PhD <sup>a</sup>, Cathrine Saxhaug MD <sup>b</sup>, Oliver Geier PhD <sup>a</sup>, Edmund Reitan MSc <sup>b</sup>, Dag Ottar Sætre MD <sup>c</sup>, Birger Breivik MD <sup>d</sup>, Timothy Reese PhD <sup>e</sup>, Kari Dolven Jacobsen MD, PhD <sup>f</sup>, Åslaug Helland MD, PhD <sup>f</sup>, Kyrre Eeg Emblem PhD <sup>a</sup>

<sup>a</sup> Department of Diagnostic Physics, Oslo University Hospital, Oslo, Norway

<sup>b</sup> Department of Radiology and Nuclear Medicine, Oslo University Hospital, Oslo, Norway

<sup>c</sup> Department of Radiology, Østfold Hospital Trust, Kalnes, Norway

<sup>d</sup> Department of Radiology, Hospital of Southern Norway, Kristiansand, Norway

<sup>e</sup> Athinoula A. Martinos Center for Biomedical Imaging, Department of Radiology, Massachusetts General Hospital, Harvard Medical School, Boston, Massachusetts

<sup>f</sup> Department of Oncology, Oslo University Hospital, Oslo, Norway

Received 26 March 2018; received in revised form 8 May 2018; accepted 14 May 2018

## Abstract

**Purpose:** This study aimed to investigate the hemodynamic status of cerebral metastases prior to and after stereotactic radiation surgery (SRS) and to identify the vascular characteristics that are associated with the development of pseudoprogression from radiation-induced damage with and without a radionecrotic component.

**Methods and materials:** Twenty-four patients with 29 metastases from non-small cell lung cancer or malignant melanoma received SRS with dose of 15 Gy to 25 Gy. Magnetic resonance imaging (MRI) scans were acquired prior to SRS, every 3 months during the first year after SRS, and every 6 months thereafter. On the basis of the follow-up MRI scans or histology after SRS, metastases were classified as having response, tumor progression, or pseudoprogression. Advanced perfusion MRI enabled the estimation of vascular status in tumor regions including fractions of abnormal vessel architecture, underperfused tissue, and vessel pruning.

Conflicts of interest: Dr. Kyrre E. Emblem has received grants from the European Union's Horizon 2020 programme, South-Eastern Norway Regional Health Authority and The Norwegian Cancer Society and holds intellectual property rights for NordicNeuroLab AS in Bergen, Norway. The remaining authors declare no conflicts of interest.

Sources of support: This project has received funding from the European Research Council (ERC) under the European Union's Horizon 2020 research and innovation programme (grant agreement No 758657), as well as the South-Eastern Norway Regional Health Authority Grants 2016102 and 2013069 and The Norwegian Cancer Society Grant 6817564.

\* Corresponding author. Department of Diagnostic Physics, The Intervention Centre, Oslo University Hospital, Building 20 Gaustad, P.O. Box 4959 Nydalen, N-0424 Oslo, Norway.

E-mail address: [ingrid.digernes@rr-research.no](mailto:ingrid.digernes@rr-research.no) (I. Digernes).

<https://doi.org/10.1016/j.adro.2018.05.005>

2452-1094/© 2018 The Author(s). Published by Elsevier Inc. on behalf of the American Society for Radiation Oncology. This is an open access article under the CC BY-NC-ND license (<http://creativecommons.org/licenses/by-nc-nd/4.0/>).

**Results:** Prior to SRS, metastases that later developed pseudoprogression had a distinct poor vascular function in the peritumoral zone compared with responding metastases ( $P < .05$ ; number of metastases = 15). In addition, differences were found between the peritumoral zone of pseudoprogressing metastases and normal-appearing brain tissue ( $P < .05$ ). In contrast, for responding metastases, no differences in vascular status between peritumoral and normal-appearing brain tissue were observed. The dysfunctional peritumoral vasculature persisted in pseudoprogressing metastases after SRS.

**Conclusions:** Our results suggest that the vascular status of peritumoral tissue prior to SRS plays a defining role in the development of pseudoprogression and that advanced perfusion MRI may provide new insights into patients' susceptibility to radiation-induced effects.

© 2018 The Author(s). Published by Elsevier Inc. on behalf of the American Society for Radiation Oncology. This is an open access article under the CC BY-NC-ND license (<http://creativecommons.org/licenses/by-nc-nd/4.0/>).

## Introduction

Cerebral metastasis is the most common intracranial malignancy in adults and the incidence of metastatic relapse increases with the improved management of primary tumors.<sup>1</sup> Stereotactic radiation surgery (SRS) is an important treatment option for patients with brain metastases.<sup>2</sup> However, SRS can cause nontumoral radiation-induced effects such as pseudoprogression and radionecrosis, which are characterized by similar features on magnetic resonance imaging (MRI) as tumor progression.<sup>3</sup> The term radionecrosis is sometimes used to describe a more severe tissue reaction than pseudoprogression.<sup>4,5</sup> However, pseudoprogression and radionecrosis are used interchangeably in the literature; therefore, we use pseudoprogression as a collective term for radiation-induced effects both with and without a radionecrotic component.

Clinical variables that are associated with the development of pseudoprogression after SRS of brain metastases include the volume of brain receiving a specific dose and pre-treatment lesion size.<sup>6,7</sup> Nevertheless, why metastases (even of similar size and receiving the same SRS-dose) respond differently to the treatment remains unknown. Moreover, little attention is given to tissue regions that surround the metastases regardless of the valuable information this peritumoral microenvironment holds.<sup>8</sup> Because pseudoprogression is believed to arise from irradiated normal tissue rather than from the core of the tumor,<sup>9,10</sup> the characterization of the microvasculature of both tumor and peritumoral regions is highly relevant to gain insights into treatment response mechanisms of pseudoprogression.

To this end, the aim of our study was to investigate an underreported phenomenon in metastatic response monitoring: The importance of vascular function of the tumor microenvironment prior to SRS and how this relates to the development of pseudoprogression. Using *in vivo* vascular MRI, our preliminary results show that peritumoral regions of metastases that later develop pseudoprogression had a distinct dysfunctional vasculature compared with responding metastases.

## Methods and materials

### Patients

The study was approved by the regional ethics committee and hospital institutional review board and written informed consent was obtained from all patients prior to inclusion in the study. A total of 31 patients were prospectively enrolled in our ongoing study and have been included to date (TREATMENT study; [clinicaltrials.gov](http://clinicaltrials.gov) identifier: NCT03458455). The TREATMENT study is an observational study that addresses the need for knowledge and adequate diagnostic biomarkers in the response assessment of patients with brain metastases. To be eligible for study inclusion, patients must receive SRS for at least 1 brain metastasis measured to a minimum of 5 mm in 1 dimension, be untreated or progressive after systemic or local therapy, have confirmed non-small-cell lung cancer (NSCLC) or malignant melanoma, be  $\geq 18$  years of age; have an Eastern Cooperative Oncology Group performance status score of maximum 1, have a life expectancy  $> 6$  weeks, and have no contradictions on MRI.

Seven patients were excluded because of post-SRS events that prevented assessment of a radiologic response: Death before first follow-up ( $n = 1$ ), contrast-agent reaction ( $n = 1$ ), or lost to follow-up ( $n = 5$ ), which left 24 patients with 29 metastases from confirmed primary NSCLC (14 patients; 17 metastases) and malignant melanoma (10 patients; 12 metastases; [Suppl. Table 1](#); available as supplementary material online only at [www.practical.radonc.org](http://www.practical.radonc.org)).

Patients with  $< 6$  months of follow-up time after SRS ( $n = 1$ ) or who received immunotherapy ( $n = 6$ ) were excluded from the part of the study on radiological response assessment, which left 17 patients with 19 metastases.

### Study design

All 24 patients underwent a baseline MRI examination prior to SRS (median: 9 days prior to SRS; range: 5-15 days). This was followed by post-SRS MRI examinations

every 3 months for the first year and subsequently every 6 months until death or a maximum of 36 months. The median follow-up time for all patients was 12 months (Range: 3-30 months; [Suppl. Table 1](#)).

SRS was delivered using a frameless, linear, accelerator-based system with dynamic conformal arcs. For patient immobilization, a commercial stereotactic mask fixation system was used. Treatment planning was performed with iPlan RT Dose (v4.5.4, Brainlab AG, Munich, Germany). The gross tumor volume was delineated on postcontrast T1-weighted images that were fused with computed tomography images and the planning target volume was generated by adding a 2-mm margin to the gross tumor volume. Depending on the tumor size, proximity to the organs at risk, and clinical status of the patient, the radiosurgical dose varied from 15 Gy to 25 Gy ([Suppl. Table 1](#)). Doses were prescribed to cover at least 99% of the planning target volume.

### Magnetic resonance imaging protocol

All MRI examinations were performed on a 3T Skyra (Siemens Healthineers, Erlangen, Germany). The MRI protocol included 3-dimensional T1-weighted images before and after contrast agent injection, fluid attenuated inversion recovery (FLAIR), diffusion weighted imaging; and gradient echo (GE)-spin echo (SE) dynamic susceptibility contrast (DSC) imaging where a shorter echo time for GE was used for brain metastases from malignant melanomas to account for potential more hemorrhage compared with those from NSCLC ([Suppl. Methods](#)). Of note, none of the metastases from malignant melanoma showed apparent signs of hemorrhage in the form of hyperintensities on pre-contrast T1-weighted images.

### Tumor outlining and radiological response assessment

The metastases were manually outlined on the postcontrast T1-weighted images by a radiologist with 12 years of experience. The associated regions of edema that surrounded the metastases were outlined on FLAIR-images. All delineations were performed using nordicICE (NordicNeuroLab AS, Bergen, Norway).

The radiologist retrospectively classified the metastases ( $n = 19$ ) as follows: Response ( $n = 7$ ) if the metastasis showed no signs of progression; pseudoprogression ( $n = 8$ ) if the size of the metastasis decreased or stabilized after an initial increase ( $n = 6$ ) or if 2 independent radiologists both interpreted the apparent growth as nontumoral ( $n = 1$ ) or histologically confirmed ( $n = 1$ ); tumor progression ( $n = 3$ ) if the imaging changes were indicative of tumorous tissue ( $n = 2$ ) or histologically confirmed ( $n = 1$ ); and inconclusive ( $n = 1$ ) if the imaging changes could not be differentiated between pseudoprogression and tumor progression.

### Image processing

DSC data from both GE and SE acquisitions were used to generate maps of cerebral blood volume, cerebral blood flow, mean transit time, and a binary mask of normal-appearing brain tissue as previously described.<sup>11,12</sup> SE-derived maps represent the microvascular characteristics and maps derived from GE are macrovascular-weighted.<sup>13</sup> Apparent diffusion coefficient maps from diffusion MRI, postcontrast T1-weighted images, FLAIR images, and associated regions of interest (ROIs) were co-registered to the DSC space using normalized mutual information co-registration. Motion correction, perfusion analysis, and co-registration were performed in nordicICE. Voxel-wise vessel architectural imaging analysis was performed in Matlab (MathWorks Inc., Natick, MA) as previously described,<sup>14</sup> which enables estimations of vessel caliber (slope) and architecture (vortex area/long axis; a marker of abnormal vasculature).

Peritumoral ROIs were created by a 4-mm wide dilation of the co-registered tumor ROIs in Matlab. The margin of 4 mm to define the peritumoral region was chosen to encompass a narrow segment around the tumor and still include an appropriate number of voxels in the ROI. Pure vasogenic edema and peritumoral and tumor ROIs were subtracted from the normal-appearing brain mask (reference tissue) and peritumoral and tumor ROIs were subtracted from the edema ROI. All perfusion maps were normalized to reference tissue.<sup>11</sup>

### Image and statistical analyses

The dysfunctional vascular characteristics were identified as follows: First, the normal range of values for each parameter was defined by the 20<sup>th</sup> and 80<sup>th</sup> percentile in the pre-treatment reference tissue across all patients. Second, poor vascular function was identified by values below/above these normal ranges: Underperfused tissue with cerebral blood flow values <20<sup>th</sup> percentile, abnormal vessels with vessel architecture values >80<sup>th</sup> percentile, microvessel pruning with microvascular blood volume <20<sup>th</sup> percentile, and macrovessel pruning with macrovascular blood volume <20<sup>th</sup> percentile.

Finally, the fraction of voxels in each ROI with these characteristics was calculated. A minimum of 9 non-zero voxels within the ROIs were chosen as a threshold for inclusion in the analysis. To account for potential confounding factors, vascular characteristics and/or treatment outcomes were also compared on the basis of cancer type (malignant melanoma/NSCLC), previous whole brain radiation therapy, and pre-treatment tumor size. To investigate the impact of pre-treatment tumor size, vascular characteristics were compared between large ( $n = 7$ ) and small ( $n = 8$ ) metastases defined as above/below the median tumor volume (1.34 cm<sup>3</sup>) of the responding and pseudoprogressing metastases.

Comparisons across the treatment outcome groups were made using Mann-Whitney U-tests and comparisons between ROIs and the reference tissue were made using Wilcoxon Signed Rank tests. Nonparametric tests were chosen due to the sample size and the distribution of the data. All statistical analyses were performed using MatLab. A *P*-value of .05 was considered significant after potential Holm-Bonferroni corrections in cases of multiple comparisons.

## Results

### Vascular function prior to stereotactic radiation surgery

The mean tumor volume prior to SRS across all 29 metastases was 3.76 cm<sup>3</sup> (Range, 0.03-28.9 cm<sup>3</sup>; [Suppl. Table 1](#)) and decreased at 3 to 9 months post-SRS (*P* < .01; all timepoints) relative to the volume at baseline. Mean edema

volume prior to SRS was 20.6 cm<sup>3</sup> (Range, 0-153.7 cm<sup>3</sup>; [Suppl. Table 1](#)) and displayed a decrease at 6 months (*P* < .05) and 9 months (*P* < .01) after SRS.

The vascular status prior to SRS of the tumor (I), peritumoral (II), and edema (III) regions are shown in [Figure 1](#). In the tumor region, the median fraction of abnormal vessels was 23% and underperfused tissue 12%. The median fraction of macro- and microvessel pruning were 9% and 29%, respectively ([Fig 1c](#)). In the peritumoral region, the median fraction of these vascular parameters was approximately 25% ([Fig 1d](#)) and in the pure edematous regions between 47% and 75%, which is probably due to the vasogenic tissue ([Fig 1e](#)).

### Poor pre-treatment vascular profiles associated with pseudoprogression

After the exclusion of patients with <6 months of follow-up time, patients who received additional immunotherapy or those who had inconclusive radiological changes, 17 pa-

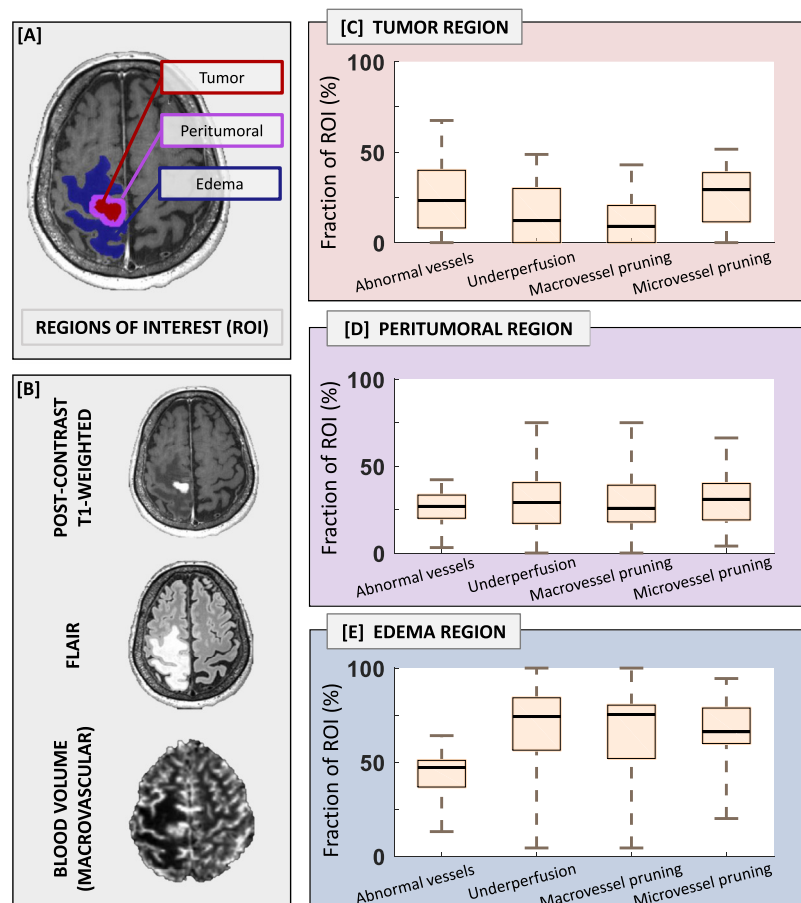


**Figure 1** Vascular characteristics prior to stereotactic radiation surgery across all patients. (a) Representative regions of interest of the tumor (red overlay), peritumoral (purple overlay), and pure edema (blue overlay) regions are shown in a patient with metastasis from non-small cell lung cancer. (b) Corresponding images of post-contrast T1-weighted, FLAIR, and blood volume-maps in the same patient. Median fractions of abnormal vessels, underperfused tissue, and macro- and microvessel pruning across all patients by tumor region (c), peritumoral region (d), and edema region (e). Boxplots (median values with interquartile range).

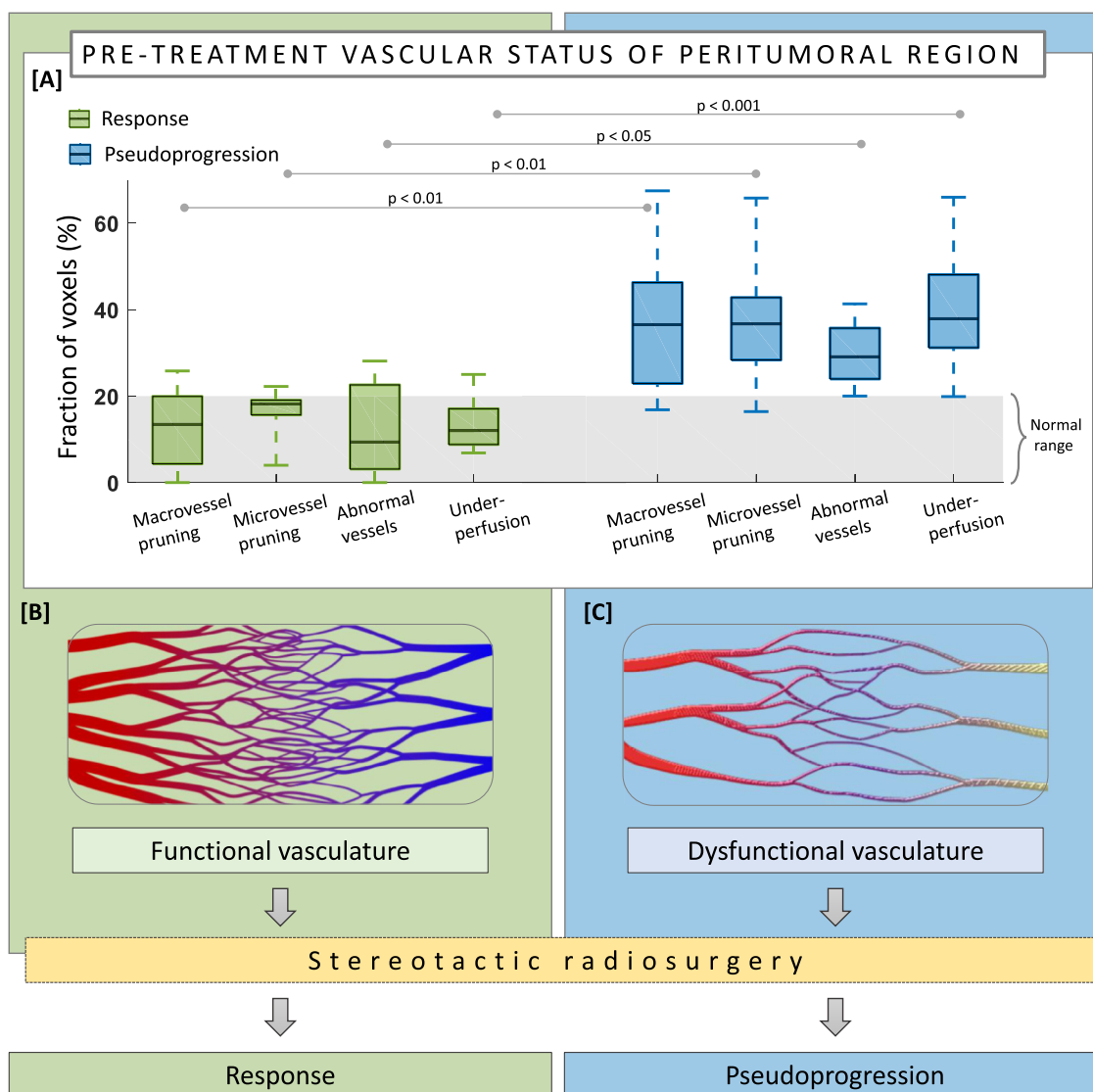


**Figure 2** Poor vascular function associated with development of pseudoprogression. (a) When compared with responding metastases (green boxes), metastases that later developed pseudoprogression (blue boxes) displayed a higher fraction of macrovesSEL pruning (13% vs 37%;  $P < .01$ ), microvesSEL pruning (18% vs 37%;  $P < 0.01$ ), abnormal vesSels (9% vs 29%;  $P < .05$ ), and underperfused tissue (12% vs 38%;  $P < .001$ ). Schematic illustration of functional pre-treatment vasculature found in responding metastases (b) compared with dysfunctional vasculature observed in metastases developing pseudoprogression (c). Boxplots (median with interquartile range);  $P$ -values from Mann-Whitney U test; [Suppl. Table 2](#).

tients with 18 metastases remained and were classified as responding ( $n = 7$ ), pseudoprogressing ( $n = 8$ ), and tumor progressing ( $n = 3$ ) lesions. When comparing the pre-SRS vascular profiles of responding lesions with those that showed pseudoprogression, we found pronounced differences in the peritumoral regions (Fig 2). Specifically, a higher fraction of both macro- and microvesSEL pruning was found in metastases that later develop pseudoprogression compared with the responding metastases. In addition, the median fraction of abnormal vesSels and underperfused tissue was more than 3-fold higher in pseudoprogressing metastases.

The fractions of micro- and macrovesSEL pruning, abnormal vesSels, and underperfused tissue in pseudoprogressing metastases were also higher compared with normal-appearing brain tissue ( $P < .05$  for all parameters). In contrast, the corresponding fractions in responding metastases were within the normal range (Fig 2, [Suppl. Table 2](#); available as supplementary material online only at [www.practical.radonc.org](http://www.practical.radonc.org)).

Interestingly, the vascular differences between pseudoprogression and responding metastases were observed in the peritumoral regions and not within the tumor core ([Suppl. Fig 1](#); available as supplementary material online only at [www.practical.radonc.org](http://www.practical.radonc.org)) nor in the pure

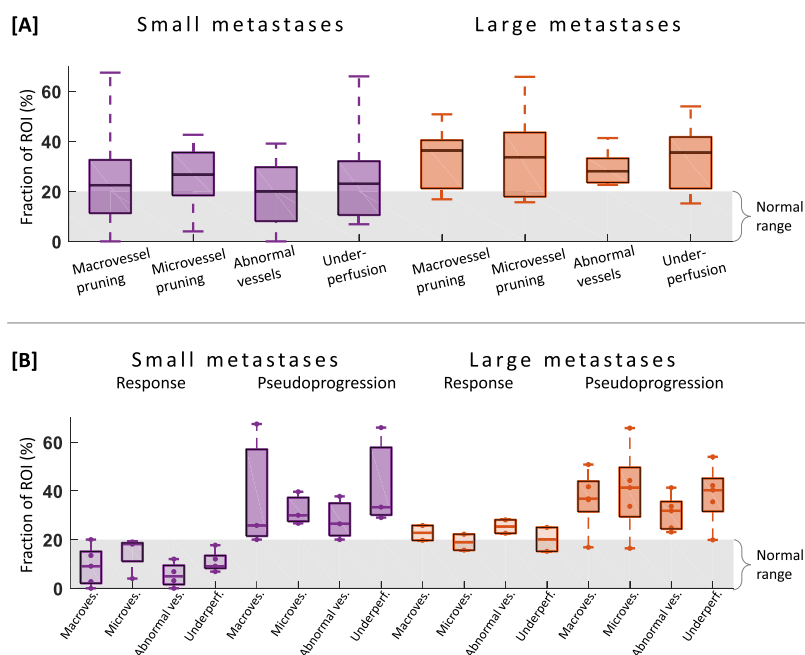


**Figure 3** Vascular profiles related to pre-treatment tumor size and treatment outcome. (a) When compared with small metastases (purple boxes), large metastases (orange boxes) displayed a trend (non-significant) toward a higher fraction of macrovessel pruning (23% vs 36%;  $P$ -value not significant on the basis of Mann-Whitney U test), microvessel pruning (27% vs 34%; not significant), abnormal vessels (20% vs 28%; not significant), and underperfused tissue (23% vs 35%; not significant). (b) Within the group of small metastases (left), the responders displayed fractions within the normal range while higher fractions were generally observed in metastases that developed pseudoprogression. Similarly, for large metastases (right), a trend toward higher fractions was observed in pseudoprogressing metastases compared with responding metastases. Of note, no statistical test was performed due to the low number of metastases in each group. Boxplots (median with interquartile range); purple/orange dots (individual metastases).

edematous regions. In contrast to the responding metastases, the peritumoral vascular profile of metastases with tumor progression was comparable to those with pseudoprogression (Suppl. Fig 2; available as supplementary material online only at [www.practical.radonc.org](http://www.practical.radonc.org)).

We found no association with previous whole-brain radiation therapy (only 1 patient), between cancer type (malignant melanoma/NSCLC) and pre-treatment vascular characteristics (Suppl. Fig 3; available as supplementary material online only at [www.practical.radonc.org](http://www.practical.radonc.org)) nor between cancer type and development of pseudoprogression ( $P = .57$ ; Fisher's exact test). Including or excluding metastases with tumor progression in the nonpseudoprogression group did not influence our results. There was no apparent association between the anatomic location of the metastases and treatment outcomes (Suppl. Table 3; available as supplementary material online only at [www.practical.radonc.org](http://www.practical.radonc.org)). The median prescribed dose to metastases that developed pseudoprogression was lower than the dose to the responding metastases (18 vs 25 Gy;  $P < .05$ ).

The median pre-treatment lesion size was 5.3 cm<sup>3</sup> in pseudoprogressing metastases compared with 0.8 cm<sup>3</sup> in responding metastases but the difference was not significant. When comparing vascular profiles of large and small metastases, the large metastases had a slight tendency toward a more dysfunctional vascularity compared with the small metastases but no significant differences were found (Fig 3a).

When examining the differences between pseudoprogression and response within the groups of small and large metastases, a stratification of vascular characteristics was observed. For small metastases ( $\leq 1.34$  cm<sup>3</sup>), pseudoprogression occurred when the peritumoral region was characterized by poor vascular function (Fig 3b, left). Correspondingly, among the large lesions ( $> 1.34$  cm<sup>3</sup>), responding metastases had generally better pre-treatment vascular function than pseudoprogressing metastases (Fig 3b, right). Finally, large responding metastases had generally poorer vascular function compared with those of small responding metastases.

### Poor function in feeding vasculature is maintained after stereotactic radiation surgery

The differences in peritumoral vascular function between pseudoprogressing and responding metastases prior to SRS were generally maintained after SRS. Higher fractions of abnormal vessels (Fig 4a), underperfused tissue (Fig 4b), and macrovessel pruning (Fig 4c) were found in metastases that developed pseudoprogression at 3 to 6 months after SRS. This was not observed for microvessel pruning (Fig 4d).

Furthermore, the fractions of abnormal vessels, underperfused tissue, and macrovessel pruning after SRS were found to be higher in the peritumoral region of

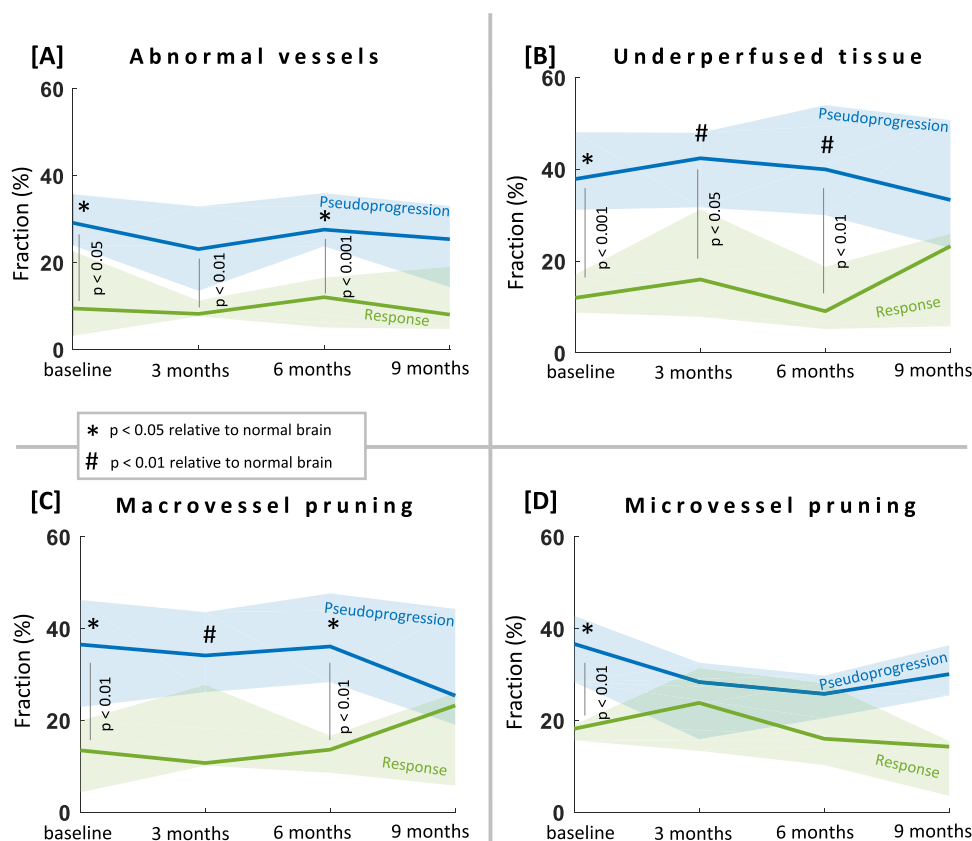


**Figure 4** Vascular signature of peritumoral zone is maintained after stereotactic radiation surgery (SRS). (a) For metastases that developed pseudoprogression, the fraction of abnormal vessels was higher than for responders at 3 months ( $P < .01$ ) and 6 months after SRS ( $P < .001$ ) and compared with normal brain tissue at 6 months ( $P < .05$ ). (b) The fraction of underperfused tissue was higher in pseudoprogressing metastases compared with responding metastases at 3 months ( $P < .05$ ) and 6 months ( $P < .01$ ) and compared with normal brain tissue ( $P < .01$ ). (c) The fraction of macrovessel pruning was higher in pseudoprogressing metastases compared with responding metastases at 6 months ( $P < .01$ ). The same trend was displayed at 3 months ( $P < .05$ ; not significant on the basis of Mann Whitney U test and after Holm-Bonferroni correction). The fraction in pseudoprogressing metastases was also higher compared with that of normal brain tissue ( $P < .01$  at 3 months;  $P < .05$  at 6 months). (d) No significant differences in the fraction of microvessel pruning were observed after SRS. Lines with transparent field (median  $\pm$  interquartile range);  $P$ -values from Mann Whitney U test (between groups) and Wilcoxon Signed Rank test (relative to normal brain).

pseudoprogressing metastases compared with normal-appearing brain tissue. In contrast, no difference between the peritumoral regions and normal-appearing brain tissue was found at any time point after SRS in responding metastases.

## Discussion

Pre-treatment vascular characteristics in brain metastases and their role in pseudoprogression is an underreported concept in clinical oncology. Human imaging data from MRI or positron emission tomography are mainly limited to post-SRS imaging and the focus of these studies have been to discriminate pseudoprogression from tumor progression after the radiological changes have occurred.<sup>15-19</sup> In contrast, our study investigated the microvascular environment of brain metastases both prior to and after SRS. Our results show

that treatment-naïve brain metastases that later develop pseudoprogression were characterized by low vascular function and supply. Our findings indicate that a high fraction of micro- and macrovessel pruning as well as underperfused tissue and abnormal vessels in the peritumoral region contribute to the development of pseudoprogression. After SRS, the observed poor vascular function of pseudoprogressing metastases continued to deviate from responding metastases as well as from normal-appearing brain tissue.

Although the exact mechanisms behind the development of pseudoprogression are not fully understood, radiation-induced damage to blood vessels and endothelial cells have been suggested to lead to increased permeability, vessel wall thickening, and occlusion.<sup>4</sup> In light of our results, the poor vascular function of pseudoprogressing metastases may indicate that the peritumoral tissue of these metastases do not have the vascular infrastructure and function necessary to tolerate the

tissue damage from SRS.<sup>20,21</sup> With a well-perfused peritumoral supply, the vascular bed may be capable of recovery after irradiation and thereby less susceptible for the development of blood vessel damage, demyelination, and ultimately pseudoprogression.

Our findings show pseudoprogression in metastases with inherent poor vascular function and supply and are in line with those from the study by Ohguri et al. where the use of hyperbaric oxygen treatment after SRS reduced the incidence of pseudoprogression.<sup>22</sup> Their study suggests that increasing the oxygen concentration in the brain parenchyma stimulates and restores blood supply that is affected by radiation-induced vascular injury and thus prevents pseudoprogression. Pseudoprogression after SRS is also linked to the volume of normal brain that receives a specific dose and thereby compromises the tissue's ability to recover.<sup>6,23-25</sup> However, Chin et al. demonstrated a large overlap in dose volumes in pseudoprogressing and nonpseudoprogressing lesions and revealed both patient and lesion-specific thresholds of irradiated volume for the development of pseudoprogression.<sup>26</sup>

In our study, metastases developing pseudoprogression were generally larger before the SRS-treatment than those of the responding metastases but with considerable overlap. This is in concordance with previous work where pre-treatment lesion size has been identified as a risk factor for pseudoprogression by some<sup>6,7</sup>, but not by others.<sup>25,27</sup> Interestingly, our findings suggest that the lesion's susceptibility to pseudoprogression is dictated by peritumoral vascular function rather than lesion size. Specifically, our results show that smaller and possibly lower at-risk metastases that developed pseudoprogression were characterized by an inherent poor vascular function. Conversely, larger metastases that did *not* develop pseudoprogression had a more functional vasculature than their pseudoprogressing counterparts. However, with few metastases in each group, there is an uncertainty related to these findings. Moreover, although only a weak association was found in our preliminary data, it is likely that there is a connection between lesion size and peritumoral vascular function. With the aggressive nature of brain metastases, larger metastases will have a greater impact on the surrounding tissue than the smaller metastases, that are likely to cause poor vascular function in peritumoral regions.

The distinct vascular profiles between the groups were observed in the peritumoral regions but not in the tumor regions. The lack of pronounced vascular differences in the tumor regions may be attributed to the lower number of voxels in the tumor ROIs, as some of the tumor ROIs were too small to be included in the analysis ( $\leq 9$  voxels), which led to fewer metastases in each group and thus made the analysis less robust. However, there was a more pronounced overlap in the vascular data between pseudoprogression and response in the tumor region compared with the peritumoral region. This may indicate that the strongest association between development of

pseudoprogression and vascular status is found in the feeding peritumoral tissue. This is in line with studies that suggest that pseudoprogression originates from the peritumoral zone<sup>9</sup> as well as histological examinations that show vascular endothelial growth factor-producing cells and astrogliosis in the peritumoral tissue.<sup>28</sup>

In our data, we did not find any associations between cancer type and pre-treatment vascular characteristics nor did the metastases from malignant melanoma show any apparent signs of hemorrhage. Given the known hemorrhagic disposition of melanomas, the occurrence of hemorrhage is likely to increase in a different cohort and could potentially affect our findings with regard to cancer type and vascular characteristics.

A limitation to our study is the small sample size. Moreover, there is an uncertainty associated with the grouping of patients on the basis of treatment outcome. Two metastases were classified as pseudoprogression without a radiographic decrease after the initial increase of the enhancing lesion. One was subsequently confirmed by histology but the classification of the other lesion relied on the response evaluation from 2 independent radiologists who both came to the same conclusion. In addition, pseudoprogression may occur several years after SRS,<sup>29</sup> which makes the classification a very relevant but inherently dynamic endpoint.

This study is also limited by the small sample size of metastases with tumor progression ( $n = 3$ ). These 3 metastases displayed poor pre-treatment vascular function similar to that of the metastases that developed pseudoprogression. However, due to the small sample size, reliable conclusions are difficult to draw about this group and the implications of these findings. Moreover, in this study, SRS was performed using a frameless linear accelerator-based system; therefore, studies using Gamma Knife SRS must be performed to establish potential differences between the 2 methods with regard to our findings.

When a larger cohort becomes available, the future work of this study will include a multivariate analysis to better determine any potential confounding factors to our findings including combinations of tumor size, histology, and SRS dose. Moreover, with more patients, a stratification on the basis of reversible pseudoprogression and irreversible radionecrosis may be enabled and potentially reveal vascular differences between the different types of radiation-induced effects.

## Conclusions

Our study investigated the importance of the vascular function of brain metastases before SRS and its role in the development of pseudoprogression. Treatment-naïve metastases that were later found to develop pseudoprogression were characterized by a high fraction of underperfused tissue and abnormal vessels as well as micro- and macrovessel

pruning in the peritumoral zone. This suggests that mapping pre-treatment vascular function may provide valuable insight into the mechanisms of pseudoprogression.

## Acknowledgments

The authors thank Knut Håkon Hole at Oslo University Hospital, Oslo, Norway for the critical and constructive review of the manuscript.

## Supplementary data

Supplementary material for this article (<https://doi.org/10.1016/j.adro.2018.05.005>) can be found at [www.practicalradonc.org](http://www.practicalradonc.org).

## References

- Lin NU, Lee EQ, Aoyama H, et al. Challenges relating to solid tumour brain metastases in clinical trials, part 1: patient population, response, and progression. A report from the RANO group. *Lancet Oncol*. 2013;14:e396-e406.
- Moraes FY, Taunk NK, Marta GN, Suh JH, Yamada Y. The rationale for targeted therapies and stereotactic radiosurgery in the treatment of brain metastases. *Oncologist*. 2016;21:244-251.
- Parvez K, Parvez A, Zadeh G. The diagnosis and treatment of pseudoprogression, radiation necrosis and brain tumor recurrence. *Int J Mol Sci*. 2014;15:11832-11846.
- Walker AJ, Ruzevick J, Malayeri AA, et al. Postradiation imaging changes in the CNS: How can we differentiate between treatment effect and disease progression? *Future Oncol*. 2014;10:1277-1297.
- Brandsma D, van den Bent MJ. Pseudoprogression and pseudoresponse in the treatment of gliomas. *Curr Opin Neurol*. 2009;22:633-638.
- Minniti G, Clarke E, Lanzetta G, et al. Stereotactic radiosurgery for brain metastases: Analysis of outcome and risk of brain radionecrosis. *Radiat Oncol*. 2011;6:48.
- Kohutek ZA, Yamada Y, Chan TA, et al. Long-term risk of radionecrosis and imaging changes after stereotactic radiosurgery for brain metastases. *J Neurooncol*. 2015;125:149-156.
- Lemee JM, Clavreul A, Menei P. Intratumoral heterogeneity in glioblastoma: Don't forget the peritumoral brain zone. *Neuro Oncol*. 2015;17:1322-1332.
- Wiggenraad R, Bos P, Verbeek-de Kanter A, et al. Pseudo-progression after stereotactic radiotherapy of brain metastases: Lesion analysis using MRI cine-loops. *J Neurooncol*. 2014;119:437-443.
- Lawrence YR, Li XA, el Naqa I, et al. Radiation dose-volume effects in the brain. *Int J Radiat Oncol Biol Phys*. 2010;76:S20-S27.
- Bjornerud A, Emblem KE. A fully automated method for quantitative cerebral hemodynamic analysis using DSC-MRI. *J Cereb Blood Flow Metab*. 2010;30:1066-1078.
- Digernes I, Bjornerud A, Vatnehol SAS, et al. A theoretical framework for determining cerebral vascular function and heterogeneity from dynamic susceptibility contrast MRI. *J Cereb Blood Flow Metab*. 2017;37:2237-2248.
- Weisskoff RM, Zuo CS, Boxerman JL, Rosen BR. Microscopic susceptibility variation and transverse relaxation: Theory and experiment. *Magn Reson Med*. 1994;31:601-610.
- Emblem KE, Mouridsen K, Bjornerud A, et al. Vessel architectural imaging identifies cancer patient responders to anti-angiogenic therapy. *Nat Med*. 2013;19:1178-1183.
- Cicone F, Minniti G, Romano A, et al. Accuracy of F-DOPA PET and perfusion-MRI for differentiating radionecrotic from progressive brain metastases after radiosurgery. *Eur J Nucl Med Mol Imaging*. 2015;42:103-111.
- Mitsuya K, Nakasu Y, Horiguchi S, et al. Perfusion weighted magnetic resonance imaging to distinguish the recurrence of metastatic brain tumors from radiation necrosis after stereotactic radiosurgery. *J Neurooncol*. 2010;99:81-88.
- Barajas RF, Chang JS, Sneed PK, Segal MR, McDermott MW, Cha S. Distinguishing recurrent intra-axial metastatic tumor from radiation necrosis following gamma knife radiosurgery using dynamic susceptibility-weighted contrast-enhanced perfusion MR imaging. *AJNR Am J Neuroradiol*. 2009;30:367-372.
- Huang J, Wang AM, Shetty A, et al. Differentiation between intra-axial metastatic tumor progression and radiation injury following fractionated radiation therapy or stereotactic radiosurgery using MR spectroscopy, perfusion MR imaging or volume progression modeling. *Magn Reson Imaging*. 2011;29:993-1001.
- Tomura N, Kokubun M, Saginoya T, Mizuno Y, Kikuchi Y. Differentiation between treatment-induced necrosis and recurrent tumors in patients with metastatic brain tumors: Comparison among 11C-methionine-PET, FDG-PET, MR permeability imaging, and MRI-ADC-preliminary results. *AJNR Am J Neuroradiol*. 2017;38:1520-1527.
- Colliez F, Gallez B, Jordan BF. Assessing tumor oxygenation for predicting outcome in radiation oncology: A review of studies correlating tumor hypoxic status and outcome in the preclinical and clinical settings. *Front Oncol*. 2017;7:10.
- Brown JM, Carlson DJ, Brenner DJ. The tumor radiobiology of SRS and SBRT: Are more than the 5 R's involved? *Int J Radiat Oncol Biol Phys*. 2014;88:254-262.
- Ohguri T, Imada H, Kohshi K, et al. Effect of prophylactic hyperbaric oxygen treatment for radiation-induced brain injury after stereotactic radiosurgery of brain metastases. *Int J Radiat Oncol Biol Phys*. 2007;67:248-255.
- Blonigen BJ, Steinmetz RD, Levin L, Lamba MA, Warnick RE, Breneman JC. Irradiated volume as a predictor of brain radionecrosis after linear accelerator stereotactic radiosurgery. *Int J Radiat Oncol Biol Phys*. 2010;77:996-1001.
- Korytko T, Radivoyevitch T, Colussi V, et al. 12 Gy gamma knife radiosurgical volume is a predictor for radiation necrosis in non-AVM intracranial tumors. *Int J Radiat Oncol Biol Phys*. 2006;64:419-424.
- Ohtakara K, Hayashi S, Nakayama N, et al. Significance of target location relative to the depth from the brain surface and high-dose irradiated volume in the development of brain radionecrosis after micromultileaf collimator-based stereotactic radiosurgery for brain metastases. *J Neurooncol*. 2012;108:201-209.
- Chin LS, Ma L, DiBiase S. Radiation necrosis following gamma knife surgery: A case-controlled comparison of treatment parameters and long-term clinical follow up. *J Neurosurg*. 2001;94:899-904.
- Schuttrumpf LH, Niyazi M, Nachbichler SB, et al. Prognostic factors for survival and radiation necrosis after stereotactic radiosurgery alone or in combination with whole brain radiation therapy for 1-3 cerebral metastases. *Radiat Oncol*. 2014;9:105.
- Nonoguchi N, Miyatake S, Fukumoto M, et al. The distribution of vascular endothelial growth factor-producing cells in clinical radiation necrosis of the brain: Pathological consideration of their potential roles. *J Neurooncol*. 2011;105:423-431.
- Hoefnagels FW, Lagerwaard FJ, Sanchez E, et al. Radiological progression of cerebral metastases after radiosurgery: Assessment of perfusion MRI for differentiating between necrosis and recurrence. *J Neurol*. 2009;256:878-887.